Multiple Source Modeling of Low-Reynolds-Number Dissipation Rate Equation with Aids of DNS Data

Young Don Choi*†, Jong Keun Shin, Kun Ho Chun
Department of Mechanical Engineering, Korea University

The paper reports a multiple source modeling of low-Reynolds-number dissipation rate equation with aids of DNS data. The key features of the model are to satisfy the wall limiting conditions of the individual source terms in the exact dissipation rate equation using the wall damping functions. The wall damping functions are formulated in term of dimensionless dissipation length scale $l_D^+ \ (\equiv l_D(\nu\varepsilon)^{1/4}/\nu)$ and the invariants of small and large scale turbulence anisotropy tensors, $a_{ij}(=\overline{u_i u_j}/k - 2\delta_{ij}/3)$ and $e_{ij}(=\varepsilon_{ij}/\varepsilon - 2\delta_{ij}/3)$. The model constants are optimized with aids of DNS data in a plane channel flow. Adopting the dissipation length scale as a parameter of damping function, the applicabilities of k-ε model are extended to the turbulent flow calculation of complex flow passages.

Key Words : Turbulence Model, Low-Reynolds-Number Dissipation Rate Equation, DNS, Dissipation Length Scale

Nomenclature ─────────────

A : Flatness parameter, $(\equiv 1 - 9(A_2 - A_3)/8)$

A_2 : Second invariant of Reynolds-stress anisotropy $(\equiv a_{ij}a_{ji})$

A_3 : Third invariant of Reynolds-stress anisotropy $(\equiv a_{ij}a_{jk}a_{ki})$

a_{ij} : Reynolds stress anisotropy tensor $(\equiv \overline{u_i u_j}/k - 2\delta_{ij}/3)$

C_d, C_D : Model coefficients in length scale

$C_{d1}, C_{d2}, C_{d3}, C_{d4}, C_{d5}$: Model coefficients used in ε equation

$C_{\varepsilon 1}, C_{\varepsilon 2}, C_{\varepsilon 3}, C_{\varepsilon 4}, C_{\varepsilon 5}$: Model coefficients used in ε equation

$C_{\varepsilon 1}^*, C_{\varepsilon 2}^*$: Equivalence model coefficients used in ε equation

D_ε : Viscous diffusion term in ε equation

E : Flatness parameter, $(\equiv 1 - 9(E_2 - E_3)/8)$

E_2 : Second invariant of dissipation rate $(\equiv e_{ij}e_{ji})$

E_3 : Third invariant of dissipation rate $(\equiv e_{ij}e_{jk}e_{ki})$

e_{ij} : Anisotropy of dissipation rate tensor $(\equiv \varepsilon_{ij}/\varepsilon - 2\delta_{ij}/3)$

f_{A2}, f_{A5} : Amplification function

$f_{d2}, f_{d3}, f_{d4}, f_{d5}$: Wall damping functions

$f_{\varepsilon t}$: Empirical function of turbulence Reynolds number

f_{w1}, f_{w2} : Transition functions

k : Turbulent kinetic energy

l_A : Modified dissipation length scale $(\equiv C_D A^{1/2}k^{3/2}/\varepsilon)$

L_D : Dissipation length scale$(\equiv C_D k^{3/2}/\varepsilon)$

l_D : Modified dissipation length scale

l_d : Dissipation length scale $(\equiv \sqrt{C_d \nu k/\varepsilon})$

l_D^+ : Dimensionless dissipation length scale$(l_D(\nu\varepsilon)^{1/4}/\nu)$

n_i : Unit vector normal to wall

P_k : Production rate of turbulent kinetic energy

† First Author
* Corresponding Author,
 E-mail : ydchoi@kuccnx.korea.ac.kr
 TEL : +82-2-3290-3355 ; **FAX :** +82-2-928-1067
 Department of Mechanical Engineering, Korea University. 1, Anam-dong, Sungbuk-ku, Seoul 136-701, Korea. (Manuscript **Received** July 22, 2000; **Revised** November 29, 2000)

$P_\varepsilon^i (i=1, 2, 3, 4)$: Production terms in ε equation

Re_τ : Channel half width Reynolds number ($\equiv U_\tau \delta / \nu$)

R_t : Turbulence Reynolds number ($k^2/ (\nu \varepsilon)$)

S : Mean strain rate

S_{ij} : Mean strain rate tensor

T_ε : Turbulent transport term in ε equation

u_i : Fluctuation component of velocity

U_i : Mean velocity tensor

U_τ : Friction velocity ($\equiv \sqrt{\tau_w / \rho}$)

y : Distance from the wall

y^+ : Dimensionless distance from the wall ($\equiv y U_\tau / \nu$)

y^* : Dimensionless distance from the wall ($\equiv y(\nu \varepsilon)^{1/4} / \nu$)

Γ : Dissipation term in ε equation

δ_{ij} : Kronecker delta

ε : Dissipation rate of turbulent kinetic energy

$\tilde{\varepsilon}$: Isotropic dissipation rate of turbulent kinetic energy

ε_w^+ : Dimensionless dissipation rate of turbulent kinetic energy at the wall

ε_{ij} : Dissipation rate of Reynolds stress

ε_{ij}^{iso} : Isotropic dissipation rate of Reynolds stress

ν, ν_t : Kinematic viscosity and eddy viscosity

Π_k, Π_ε : Pressure transport in k and ε equations

ρ : Fluid density

τ_w : Wall shear stress

χ : Von Karman's constant

1. Introduction

In many cases, applications of low-Reynolds-number k-ε model to the turbulent shear flows lead to a marked improvement over the wall functions in predicting the engineering turbulent flows[Launder(1984)]. Modeling the exact dissipation rate equation is essential for successful application of a low-Reynolds-number k-ε model to the turbulent flow calculations. Various forms for the low-Reynolds-number dissipation rate equation models have been proposed in the past, but due to the lack of detailed and reliable data for budget of the dissipation rate equation, the verifications of the models were not possible until the appearance of DNS data.

The DNS data provided the detailed and accurate budgets of the dissipation rate equation which could not be obtained from the experiments. Mansour, Kim and Moin(1988, 1989) [here after MKM] computed the budgets of the dissipation rate equation for a plane channel flow. Rodi and Mansour(1993) [here after RM] proposed a model for the exact dissipation rate equation with the aids of DNS data. They multiplied the exponential amplification function to the dissipation terms of dissipation rate equation which involved a parameter composed of a ratio of the time scale of the dissipation motion to the time scale of P_k / ε. Here P_k is the production rate of turbulent kinetic energy. Nagano and Shimada (1993) [here after NS] and Nagano, Youssef and Shimada(1993) [here after NYS] proposed the low-Reynolds-number dissipation rate equation models which yielded the dissipation rate profiles agreeing well with the DNS data. Those model employed the elaborated empirical functions for modeling source terms in dissipation rate equation.

An exact dissipation rate equation involves five source terms. However, most of previous models for the sources are based on recomposition of the sources into one production and one dissipation term. This kind of recomposition model of the sources into equivalent production and dissipation terms can be validated only in a high Reynolds number region where the production rate of turbulent kinetic energy is nearly balanced with its dissipation rate. However, approaching to the wall, the source terms behave too independently to be combined into an equivalent model form.

In the present study, the low-Reynolds-number models for the dissipation rate equation are improved by introducing a multiple source concept. The key features of the present model are to satisfy the wall limiting conditions of each source term using the wall damping functions which are

composed in terms of the invariants of anisotropy tensors of Reynolds stress $a_{ij} (=\overline{u_i u_j}/k - 2\delta_{ij}/3)$, its dissipation rate $e_{ij} (=\varepsilon_{ij}/\varepsilon - 2\delta_{ij}/3)$, and the dimensionless dissipation length scale $l_D^+ (\equiv l_D (\nu\varepsilon)^{1/4}/\nu)$.

2. Near Wall Behaviors of Exact Dissipation Rate Equation

For incompressible flow, the exact equation for dissipation rate $(\varepsilon = \nu \overline{u_{i,j} u_{i,j}})$ derived from the Navier-Stokes equations can be written in a tensor form as

$$\frac{D\varepsilon}{Dt} = P_\varepsilon^1 + P_\varepsilon^2 + P_\varepsilon^3 + P_\varepsilon^4 + T_\varepsilon + \Pi_\varepsilon + D_\varepsilon - \Gamma \quad (1)$$

where the terms on the right hand side are defined and identified as

Mixed production :
$$P_\varepsilon^1 = -2\nu \overline{u_{i,j} u_{k,j}} S_{ik} \quad (2)$$
Production by mean velocity gradient :
$$P_\varepsilon^2 = -2\nu \overline{u_{i,k} u_{i,m}} S_{km} \quad (3)$$
Gradient production :
$$P_\varepsilon^3 = -2\nu \overline{u_k u_{i,m}} U_{i,km} \quad (4)$$
Turbulent production :
$$P_\varepsilon^4 = -2\nu \overline{u_{i,k} u_{i,m} u_{k,m}} \quad (5)$$
Turbulent transport : .
$$P_\varepsilon = -\nu \overline{(u_k u_{i,m} u_{i,m,k}} \quad (6)$$
Pressure transport :
$$\Pi_\varepsilon = -2\frac{\nu}{\rho} \overline{(p_{,m} u_{k,m})_{,k}} \quad (7)$$
Viscous diffusion :
$$D_\varepsilon = \nu\varepsilon_{,kk} \quad (8)$$
Dissipation :
$$\Gamma = 2\nu^2 \overline{u_{i,km} u_{i,km}} \quad (9)$$

For a fully developed plane channel flow, the left hand side of Eq. (1) is zero so that the terms on the right hand side has to be in balanced. MKM(1988) calculated the budgets of the terms of k equation from Kim, Moin & Moser's(1989) DNS data. They compared the calculated ε budgets with the estimates obtained from Laufer's(1954) data[see Townsend(1956)], and found that they overestimated the turbulent transport and pressure diffusion terms. On the other hand, they underestimated the viscous diffusion term and resulted in a maximum value of the ε away
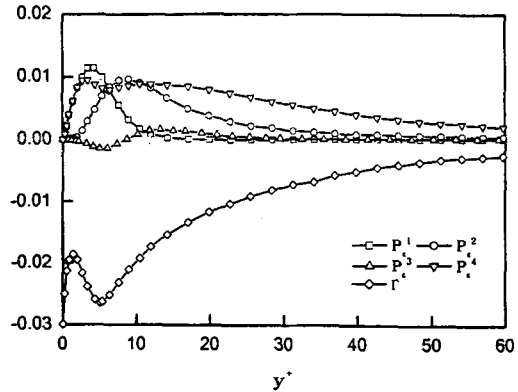

Fig. 1 Near wall budgets of ε in a plane channel flow, $Re_\tau = 395$

from the wall. Most of the low-Reynolds-number k-ε models proposed before 1990 gave the distribution of ε that reached a maximum value away from the wall[Patal, Rodi and Scheurer(1985)] as shown in Laufer's data. However the budgets from the DNS data always show the maximum of ε at the wall. This implies the necessity for a substantial modification to the dissipation rate equation model in a low Reynolds number region.

Figure 1 shows the budgets of the dissipation rate equation evaluated from the MKM's (1988) DNS data in a plane channel flow for $Re_\tau = 395$. All the terms in the figure are made dimensionless with U_τ^6/ν^2. Hanjalic and Launder(1972, 1976) [here after HL] attempted to provide approximations of the terms on the right hand side of Eq. (1) in terms of ε, $\overline{u_i u_j}$ and mean rate of the strain. They proposed the following approximation for closing $P_\varepsilon^1 + P_\varepsilon^2$.

$$P_\varepsilon^1 + P_\varepsilon^2 = C_{\varepsilon 1}^* \frac{P_k \varepsilon}{k} \quad (10)$$

where $C_{\varepsilon 1}^*$ is an equivalent model constant.

However, P_ε^1 and P_ε^2 are only important in the near wall sublayer. In a high Reynolds number region, production by vortex self-stretching and the viscous dissipation terms of ε equation dominates the dynamics of ε and balances with the transport term. Hence, the most of previous studies have concentrated their works to the identification of the net effects of the two source terms,

without considering the characteristics of individual source terms. Rodi(1971) argued that the turbulent production term P_ε^4 which expressed the self-stretching action of turbulence, should be considered in conjunction with the dissipation term Γ. HL(1972) also argued that in high Reynolds number region where the inertial subrange existed, dynamics of the energy cascade process controlled P_ε^4 and Γ. Thereafter, the difference between P_ε^4 and Γ has been modeled persistently as follows;

$$P_\varepsilon^4 - \Gamma = C_{\varepsilon2}^* \frac{\varepsilon^2}{k} \tag{11}$$

where $C_{\varepsilon2}^*$ is a equivalent model constant.

This concept is, however, too simplified to simulate the complex near wall turbulence behaviors. Therefore we attempt to develop a multiple source model of the exact dissipation rate equation so that the k-ε model can be applied to the turbulent flow calculations in the complex flow passages.

3. Proposals for the Low-Reynolds-Number ε Equation Model

In the immediate vicinity of a wall the fluctuating velocity components may be expanded in Taylor series as follows :

$$u_1 = b_1(y^+) + c_1(y^+)^2 + d_1(y^+)^3 + \cdots\cdots$$
$$u_2 = c_2(y^+)^2 + d_2(y^+)^3 + \cdots\cdots \tag{12}$$
$$u_3 = b_3(y^+) + c_3(y^+)^2 + d_3(y^+)^3 + \cdots\cdots$$

From Eq. (12) turbulence kinetic energy and its dissipation rate near the wall vary according to

$$k = a(y^+)^2 + b(y^+)^3 + \cdots\cdots \tag{13}$$
$$\varepsilon = 2a + 4b(y^+) + \cdots\cdots \tag{14}$$

where $a = (b_1^2 + b_3^2)/2$ and $b = (b_1 c_1 + b_3 c_3)$.

Then the Taylor series expansion of the turbulent kinetic energy yield the following

$$P_k = \frac{1}{2}\overline{b_1 b_{3,3}}(y^+)^3 + O[(y^+)^4] \tag{15}$$

In order to analyse the near wall asymptotic behavior of the individual terms in ε equation, MKM expanded the terms by Taylor series as follows :

$$P_\varepsilon^1 = 2\overline{b_1 b_{3,3}}(y^+) + O[(y^+)^3] \tag{16}$$
$$P_\varepsilon^2 = 4\overline{c_1 c_2}(y^+)^2 + O[(y^+)^3] \tag{17}$$
$$P_\varepsilon^3 = -\frac{1}{Re_\tau}\overline{b_1 b_{3,3}}(y^+)^2 + O[(y^+)^3] \tag{18}$$
$$P_\varepsilon^4 = 3(\overline{b_1 b_1 b_{3,3}} + \overline{b_3 b_3 b_{1,1}})(y^+) + O[(y^+)^2] \tag{19}$$
$$T_\varepsilon = (\overline{b_1 b_1 b_{3,3}} + \overline{b_3 b_3 b_{1,1}})(y^+) + O[(y^+)^2] \tag{20}$$
$$\Pi_\varepsilon = -8\overline{c_2 c_2} + O[(y^+)] \tag{21}$$
$$D_\varepsilon = 4[\overline{b_{1,1}b_{1,1}} + \overline{b_{1,3}b_{1,3}} + \overline{b_{3,3}b_{3,3}} + \overline{b_{3,1}b_{3,1}}$$
$$+ 2(\overline{c_1 c_1 + c_2 c_2 + c_3 c_3}) + 2\overline{c_2 c_2} + O[(y^+)] \tag{22}$$
$$\Gamma = 4[\overline{b_{1,1}b_{1,1}} + \overline{b_{1,3}b_{1,3}} + \overline{b_{3,3}b_{3,3}} + \overline{b_{3,1}b_{3,1}}$$
$$+ 2(\overline{c_1 c_1 + c_2 c_2 + c_3 c_3}) + O[(y^+)] \tag{23}$$

The first term on the right hand side of the above equations are the wall limiting conditions which each source term should be satisfied as approaching to the wall. One of the present contribution is to propose a multiple source model for the exact ε equation in the near wall sublayer that satisfy these wall limiting conditions.

The mixed production rate of Eq. (2) may be expressed as

$$P_\varepsilon^1 = -\varepsilon_{ik}S_{ik} = -\varepsilon_{ij}S_{ij} \tag{24}$$

If the dissipation rate of Reynolds stress ε_{ij} is known, this term needs no further approximation. The general form of the dissipation tensor is taken over from the second-moment modeling ideas[Launder and Reynolds(1983), Launder and Tselepidakis(1991)] as follows

$$\varepsilon_{ij} = (1 - f_{w1})\varepsilon_{ij}^{iso} + f_{w1}\varepsilon_{ij}^* \tag{25}$$

where $\varepsilon_{ij}^{iso} = 2/3\varepsilon\delta_{ij}$, f_{w1} is a transition function, and

$$\varepsilon_{ij}^* = \frac{\frac{\varepsilon}{k}(\overline{u_i u_j} + \overline{u_i u_k}n_k n_j + \overline{u_j u_k}n_k n_i + n_i n_j \overline{u_k u_l}n_k n_l)}{1 + \frac{3}{2}\frac{\overline{u_k u_l}}{k}n_k n_l} \tag{26}$$

where n_k is a unit normal vector from the wall.
Substituting Eqs. (25) and (26) into (24) gives

$$P_\varepsilon^1 = (1 - f_{w1})(-\frac{2}{3}\varepsilon\delta_{ij})S_{ij} - f_{w1}\varepsilon_{ij}^* S_{ij}$$
$$= f_{w1}\frac{\varepsilon}{k}(P_k - 2\overline{u_2 u_j}S_{2j})/(1 + \frac{3}{2}\frac{\overline{u_2^2}}{k}) \tag{27}$$

where subscript 2 denotes a normal direction to the wall.

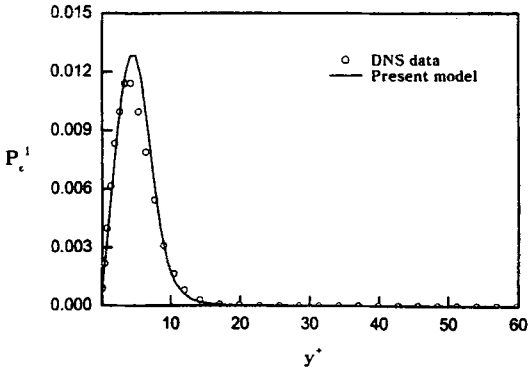Fig. 2 Model for P_ϵ^1 production compared with DNS data, $Re_\tau = 395$

Fig. 3 Distribution of parameters R and R_p in a plane channel flow, $Re_\tau = 395$

In a fully developed plane channel flow, Eq. (27) is reduced to a simple form

$$P_\epsilon^1 = [2f_{w1}/(1+\frac{3}{2}\frac{\overline{u_2^2}}{k})]\frac{P_k\epsilon}{k} = C_{\epsilon 1}\frac{P_k\epsilon}{k} \quad (28)$$

If the transition function $f_{w1} = 1 - \exp(-(R_t/C_{d1})^2)$ is taken,

$$C_{\epsilon 1} = 2[1 - \exp(-(R_t/C_{d1})^2)]/(1+\frac{3}{2}\frac{\overline{u_2^2}}{2}) \quad (29)$$

where $C_{d1} = 80$ is chosen by reference to the DNS data. $\overline{u_2^2}/2$ in the above equation can be taken from the second-moment closure of Reynolds stresses. Here in the present study it is taken from DNS data. From Eqs. (14) ~ (16), one may arrive at the wall limiting condition of $C_{\epsilon 1} = 2$ as approaching to the wall. Present model of Eq. (29) for $C_{\epsilon 1}$ satisfies this wall limiting condition exactly. Figure 2 shows the comparison of the present model for P_ϵ^1 with the budgets from DNS data for $Re_\tau = 395$. All the production terms in the following figures are normalized by U_τ^6/ν^2. Agreement between the present P_ϵ^1 model and DNS data is excellent.

Production by mean velocity gradient P_ϵ^2 can be closely related by $P_k\epsilon/k$. RM(1993) argued that the magnitude of the production terms P_ϵ^1 and P_ϵ^2 relative to the other terms in the ϵ equation model (difference $P_\epsilon^4 - \Gamma$ and transport terms) can be established as

$$\frac{P_\epsilon^1, P_\epsilon^2}{P_\epsilon^4 - \Gamma} = O\left(\frac{Sk}{\epsilon}\frac{1}{R_t^{1/2}}\right) \quad (30)$$
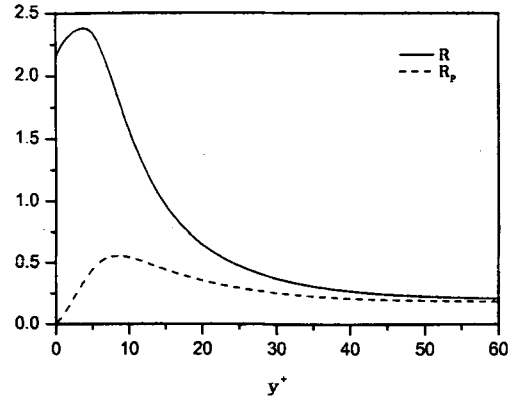
Therefore the magnitude of P_ϵ^1 and P_ϵ^2 can be determined by the parameter,

$$R = \frac{Sk}{\epsilon}\frac{1}{R_t^{1/2}} \quad (31)$$

where S was a mean strain rate and the parameter R a ratio of the time scale of the dissipation motion to that of mean strain field. They found, however, that the parameter $R_p(= (P_k/\epsilon)/0.3\,R_t^{1/2})$ obtained by replacing Sk/ϵ in Eq. (31) by P_k/ϵ might correlate better the magnitude P_ϵ^1 and P_ϵ^2 relative to the strain terms. Figure 3 shows the distribution of the parameters R and R_p calculated from the DNS data in a plane channel flow at $Re_\tau = 395$.

It has long been argued that mean shear terms had no proper place in a dissipation-rate equation since the dissipation process has been concerned with time grained turbulence[Lumley et. al. (1974)]. However, Launder(1987) argued that just as mean shear deformed the large scale eddies, so much anisotropies in the large-scale eddies was expected to stretch eddies of some what finer scale and thus contribution to the rate of energy cascade across the spectrum. This idea led the inexorable conclusion that one or both the stress invariants ought to appear in the ϵ equation.

The second and third invariants and flatness factors of the anisotropy tensors, $a_{ij}(= \overline{u_iu_j}/k - 2\delta_{ij}/3)$ of Reynolds stress $\overline{u_iu_j}$ and $e_{ij}(= \epsilon_{ij}/\epsilon - 2\delta_{ij}/3)$ of dissipation rate ϵ_{ij} are shown in Fig. 4. In this figure, large scale anisotropy invariants
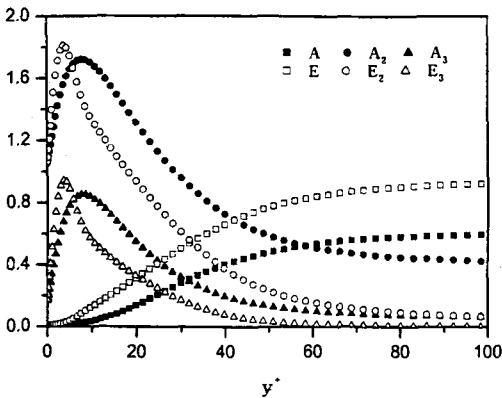
Fig. 4 Second and third invariants and flatness factors of e_{ij} and a_{ij} from DNS data
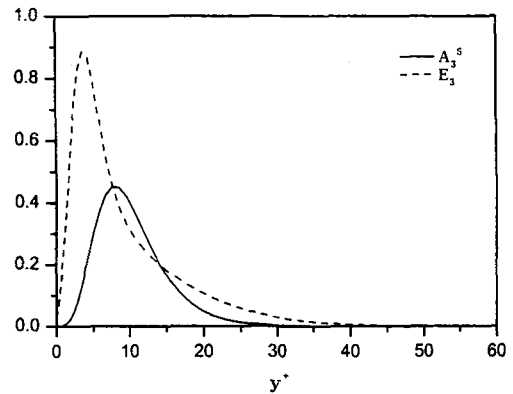

Fig. 5 Distribution of parameters A_3^s and E_3^s in a plane channel flow, $Re_\tau = 395$

$A_2 (= a_{ij}a_{ji})$ and $A_3 (= a_{ij}a_{jk}a_{ki})$ have maximum values around $y^+ = 7.5$. On the other hand, small scale anisotropy invariants $E_2 (= e_{ij}e_{ji})$ and E_3 $(= e_{ij}e_{jk}e_{ki})$ have maximum values around $y^+ = 5$ and decay faster than A_2 and A_3 away from the wall. Comparison of Figs. 3 and 4 shows that the second invariant of anisotropy tensors, A_2 and E_2 have similar shapes to that of R, and the shapes of the third invariants of anisotropy tensors, A_3 and E_3 are also similar to that of R_p. These facts imply the existence of correlation between the turbulence anisotropy and P_ε^1 and P_ε^2. Distributions of parameters $\mathbf{E_3}$ and $\mathbf{A_3^s}$ described in Fig. 5 show an obvious evidence for the existence of relationship between the third invariants of anisotropy tensors and P_ε^1 and P_ε^2, because the shapes of E_3 and A_3^s are so similar to those of P_ε^1 and P_ε^2 shown in Figs. 2 and 7. Therefore we formulated an amplification function f_{A2} in terms of A_3^s to account for the effect of large scale turbulence anisotropy on P_ε^2

$$f_{A2} = \exp(C_{A2}A_3^s) \qquad (32)$$

Wall limiting condition of Eq. (17) can be satisfied by multiplying the exponential damping function which is formulated in terms of the dimensionless distance from the wall.

$$f_{d2} = 1 - \exp(-y^+/C_{d2}) \qquad (33)$$

However, using of y^+ as a parameter of damping functions confines the applicability of the model only to the simple flow passages due to the difficulty in obtaining the y^+ in the complex flow passages.

Abe et al. [1994] proposed the use of dimensionless distance $y^* (= y(\nu\varepsilon)^{1/4}/\nu)$ to extend the applicability of their low Reynolds number k-ε model to the reattaching flows. They introduced the Kolmogrov velocity scale $(\nu\varepsilon)^{1/4}$ instead of the friction velocity U_τ to account for the near wall and low Reynolds number effects in both attached and detached flows. However, the use of y in the dimensionless distance y^* also limited the applicability of the model to the geometrically simple flow passage. Therefore, we investigate the alternative length scale which can be obtained easily even in the arbitrary flow passages.

At a high Reynolds number region, the dissipation rate is generally expressed as

$$\varepsilon = C_D k^{3/2} / L_D \qquad (34)$$

which is an outcome of dimensional analysis under the local isotropy assumption. Since the length scale $k^{3/2}/\varepsilon$ obtained from Eq. (34) is not propotional to the distance from the wall as shown in Fig. 6, Launder(1996) and Craft(1988) modified the length scale by multiplying $A^{1/2}$ where A was the flatness parameter of Lumley [1978], defined by $A = 1 - 9/8(A_2 - A_3)$ and A_2 and A_3 were the invariants of the stress anisotropy tensor, $A_2 = a_{ij}a_{ji}$, $A_3 = a_{ij}a_{jk}a_{ki}$. However, as shown in Fig. 7, the modified length scale $l_A (= C_D A^{1/2} k^{3/2}/\varepsilon)$ also departs from the linearity in the near wall sublayer.
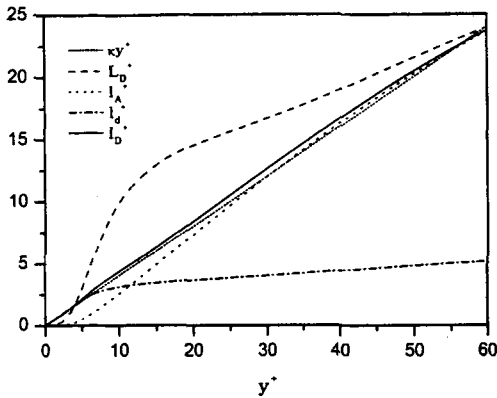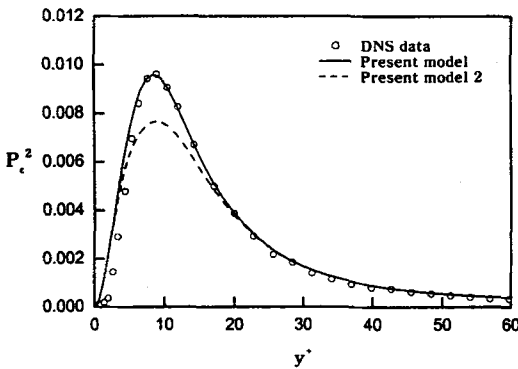
Fig. 6 Comparison of dimensionless length scales

Fig. 7 Model for P_ϵ^2 production compared with DNS data; $Re_\tau = 395$

As approaching to the wall, the dissipation rate is better expressed by the relation

$$\varepsilon = C_d \nu k / l_d^2 \qquad (35)$$

which yields the linear length scale in the near wall sublayer $y^+ \leq 6$. Applying the Launder and Craft's length scale modification to Eq. (34) and adding Eq. (35), we obtain the following total dissipation rate relation as

$$\varepsilon = C_d \frac{\nu k}{l_D^2} + C_D A^{1/2} \frac{k^{3/2}}{l_D} \qquad (36)$$

Rearranging Eq. (36), we have

$$\varepsilon l_D^2 - C_D A^{1/2} k^{3/2} l_D - C_d \nu k = 0 \qquad (37)$$

The positive root of Eq. (37) is

$$l_D = \frac{C_D k^{3/2} \left(A^{1/2} + \sqrt{A + \dfrac{4C_d}{C_D^2 R_t}} \right)}{2\varepsilon} \qquad (38)$$

We adopted $C_d = 1.7 \chi^2$ and $C_D = 1.3 C_\mu^{3/4}$ to coin-

cide the length scale l_D with the Von Karman's mixing length χy in the plane channel flow. We can replace all the y^+ in the dissipation rate equation model by the dimensionless length scale

$$l_D^+ = (l_D / \chi)(\varepsilon \nu)^{1/4} / \nu \qquad (39)$$

The l_D^+ has several attactive properties as a length scale parameter. It can easily be calculated even in the arbitrary flow passage since it does not require any normal distance from the wall and friction velocity U_τ which are very difficult to obtain in the complex flow passages.

A damping function f_{d2} in terms of a newly defined parameter l_ϵ^+ and amplification function f_{A2} are multiplied to $P_k \varepsilon / k$ to obtain the P_ϵ^2 model. The resulting form for P_ϵ^2 model is given by

$$P_\epsilon^2 = C_{\epsilon2} [(1 - \exp(- l_D^+ / C_{d2})] \exp(C_{A2} A_3^5) \frac{P_k \varepsilon}{k}$$

$$= C_{\epsilon2} f_{d2} f_{A2} \frac{P_k \varepsilon}{k} \qquad (40)$$

where $C_{\epsilon2} = 1.0$, $C_{d2} = 0.6$ and $C_{A2} = 0.5$ are adopted.

Comparison of the present P_ϵ^2 model with DNS data is shown in Fig. 7. The solid line is a profile of P_ϵ^2 predicted by the present model Eq. (40), and the dotted line is the prediction by the model $P_\epsilon^2 = C_{\epsilon2} f_{d2} P_k \varepsilon / k$ without multiplying the amplification function f_{A2}. By introducing the amplification function f_{A2}, the improved P_ϵ^2 profile can be obtained.

Eqs. (28) and (40) are added to derive a standard form of the equivalent production model as follows ;

$$P_\epsilon^1 + P_\epsilon^2 = \{2[1 - \exp(1 - (R_t / C_{d1})^2)] / [1 + 3/2 \overline{u_2^2}]$$

$$+ C_{\epsilon2} [1 - \exp(l_D^+ / C_{d2})] \exp(C_{A2} A_3^3) \} \frac{P_k \varepsilon}{k}$$

$$= C_{\epsilon1}^* \frac{P_k \varepsilon}{k} \qquad (41)$$

Numerical calculations for the plane channel flow show that the computed ε profiles are primarily influenced by the near wall behavior of $C_{\epsilon1}^*$. Lai and So (1990) [here after LS] proposed a model coefficient $C_{\epsilon1}^*$ as a function of turbulence Reynolds number R_t and Reynolds number Re_D based on the hydraulic diameter.

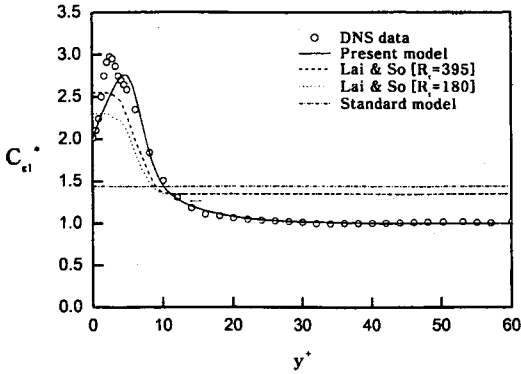Three $C_{\epsilon1}^*$ model coefficients, present model, LS

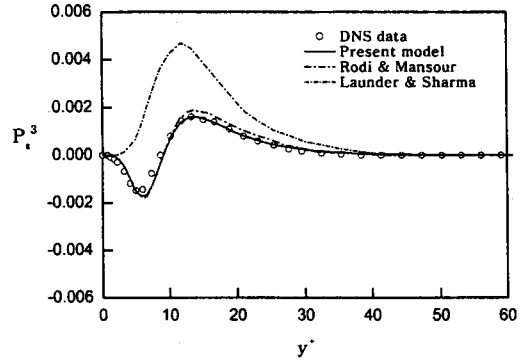**Fig. 8** Comparison of model coefficient $C_{\varepsilon 1}^*$ in a plane channel flow, $Re_\tau = 395$

Fig. 9 Model for P_ε^3 production compared with DNS data, $Re_\tau = 395$

model and standard high Reynolds number model for a fully developed turbulent channel flow are compared in Fig. 8 for $Re_\tau = 395$. The present model agrees best with the DNS data and satisfies exactly the wall limiting condition of $C_{\kappa 1}^*$ $=2.0$. It increases to the maximum value of about 2.80 near $y^+ = 4$, then decreases to the high Reynolds number value of 1.0. On the other hand, LS model gives the maximum value at the wall and decreases away from the wall to the high Reynolds number value of 1.35. Two models commonly reach to the high Reynolds number limiting values at around $y^+ = 20$. However, LS model shows the Reynolds number dependency in the maximum values $C_{\varepsilon 1}^*$. It changes from 2.30 at low Reynolds number to 2.55 at high Reynolds number.

Launder and Sharma(1974) proposed the P_ε^3 model which approximated the fluctuating velocity gradients $u_{i,j}$ in P_ε^3 in terms of a second derivative of the mean velocity. RM(1993) improved Launder & Sharma's(1974) model for P_ε^3 using the exact equation for $\overline{u_k u_{i,j}}$ appearing in P_ε^3. They added a term, which contained the first derivatives of the mean velocity and the turbulent kinetic energy as given by Eq. (42);

$$P_\varepsilon^3 = C_{\varepsilon 3}^1 \nu \nu_t \frac{k}{\varepsilon} (U_{,yy})^2 + C_\varepsilon^2 \nu \frac{k}{\varepsilon} k_{,y} U_{,y} U_{,yy}$$

(42)

The RM's model of Eq. (42) agrees very well with the DNS data, but some overprediction on the maximum and minimum values are shown in

Fig. 9. Further Eq. (42) does not satisfy the wall limiting conditions of $P_\varepsilon^3 \sim O[(y^+)^3]$ given in Eq. (18) as approaching to the wall. The wall limiting condition can be satisfied exactly by multiplying a damping function $f_{\varepsilon 3}$ to the Eq. (42).

$$P_\varepsilon^3 = f_{d3} [C_{\varepsilon 3}^1 2 \nu \nu_t \frac{k}{\varepsilon} (U_{,yy})^2$$

$$+ C_{\varepsilon 3}^2 \nu \frac{k}{\varepsilon} k_{,y} U_{,y} U_{,yy}]$$

(43)

where $f_{\varepsilon 3} = 1/[1 - \exp(-l_D^+/C_{d3})]$, $C_{\varepsilon 3} = 0.4$, $C_{\varepsilon 3}^2$ $= 0.0045$ and $C_{d3} = 0.5$. In the present study, by multiplying this damping function, overprediction of the maximum and minimum values in P_ε^3 model can be removed.

It is easy to show that the equivalence model coefficient $C_{\varepsilon 2}^*$ in Eq. (11) is proportional to $1/n$ $+1$ in a homogeneous turbulent flow which decays at a rate proportional to x^{-n}. Jones and Launder(1972) and HL(1976) multiplied the exponential damping function $f_{\varepsilon t}(R_t)$ to $C_{\varepsilon 2}^*$ to ensure the increasing effect of decaying rate of turbulence on the model $C_{\varepsilon 2}^*$ as the turbulence Reynolds number R_t decreased. Note that ε takes a non-zero value at the wall, while k vanishes, and thus the quantity ε^2/k tends to be infinite. They prevent ε^2/k from becoming infinite at the wall by replacing ε^2 by $\tilde{\varepsilon}\varepsilon$ where the quantity $\tilde{\varepsilon}$ is isotropic dissipation rate.

Equations (19) and (23) show that P_ε^4 is proportional to $O[(y^+)]$ approaching to the wall but Γ has a constant value at the wall, thus in order to simulate exactly this combined near wall
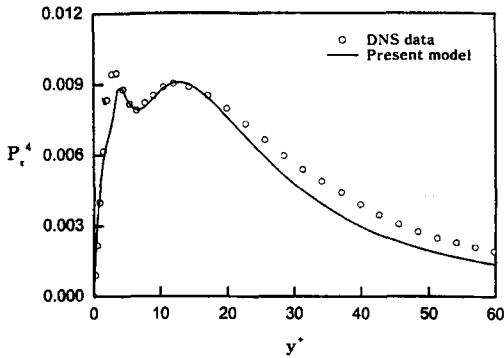
Fig. 10   Model for P_ϵ^4 production compared with DNS data, $Re_\tau = 395$

Fig. 11   Model for Γ dissipation compared with DNS data, $Re_\tau = 395$

turbulence behavior of $P_\epsilon^4 - \Gamma$, a complicated empirical modification for the model coefficients is needed. Present contribution is to propose the individual models for each P_ϵ^4 and Γ. Instead of the use of the isotropic dissipation rate $\tilde{\varepsilon}$, an exponential or hyperbolic tangent damping function is multiplied to ε^2/k to prevent the model to be diverging at the wall. The resulting model form for P_ϵ^4 is given by

$$P_\epsilon^4 = C_{\epsilon 4} f_{\epsilon t} f_{\epsilon 4} \frac{\varepsilon^2}{k} \qquad (44)$$

$$f_{\epsilon t} = 1 - 0.3 \exp[(-R_t/6)^2] \qquad (45)$$

$$f_{\epsilon 4} = [1 - \exp(-l_D^+/C_{d4})]^3 \qquad (46)$$

where $C_{\epsilon 4}$ and C_{d4} are taken as 3.1 and 1.3 respectively.

Figure 10 shows the comparison of the present model for P_ϵ^4 with DNS data for a plane channel flow for $Re_\tau = 395$. The DNS data shows a large hole in P_ϵ^4 profile around $y^+ = 6.0$. In the present model, this hole is captured very closely to that of DNS data by introducing the exponential damping function of Eq. (46).

Viscous dissipation term of ε equation can be correlated by ε^2/k. However, hyperbolic tangent damping function $f_{\epsilon 5} = \tanh^2(l_D^+/C_{d5})$ and $f_{\epsilon t} = 1 - 0.3 \exp(-(R_t/6)^2)$ are multiplied to satisfy the wall limiting condition of Eq. (23) and to ensure the increasing effect of decaying rate of ε as R_t decreases. The effects of small and large scale turbulent anisotropies on $P_{\epsilon 1}$ and $P_{\epsilon 2}$ should be balanced by the dissipation term Γ. RM account this effect by multiplying an amplification func-

tion $f_{\epsilon 5} = \exp(2R_p^2)$ to the coefficient $C_{\epsilon 2}^*$ in Eq. (12). However, since we already mentioned that R_p could be replaced by A_3 and E_3, we use $E_3 A_3^5$ as an amplification parameter which involves both effects of large and small scale turbulence anisotropies. The resulting amplification function proposed in the present study is as follows

$$f_{A5} = \exp(C_{A5} E_3 A_3^5) \qquad (47)$$

Then the final form for Γ is given by

$$\Gamma = C_{\epsilon 5} f_{\epsilon t} f_{A5} f_{d5} \frac{\varepsilon^2}{k} \qquad (48)$$

$$f_{\epsilon t} = 1 - 0.3 \exp[-(R_t/6)^2] \qquad (49)$$

$$f_{d5} = \tanh^2(l_D^+/C_{d5}) \qquad (50)$$

where $C_{\epsilon 5} = 4.58$, $C_{d5} = 1.8$ and $C_{A5} = 1.3$ are adopted.

Figure 11 shows a comparison of the present Γ profiles with DNS data. The solid line shows the present model of Eq. (48) and the long dashed line is the Γ profile obtained by replacing the parameter A_3^6 by $E_3 A_3^5$. The short dashed line is the Γ profile predicted by the model which does not multiply f_{d5}. This figure shows that the $E_3 A_3^5$ is the best choice to formulate the Γ term to be balanced with small and large scale turbulence anisotropies in P_ϵ^1 and P_ϵ^2. By subtracting Eq. (48) from Eq. (44), $P_\epsilon^4 - \Gamma$ can be combined into an equivalence dissipation model form for the ε equation.

$$P_\epsilon^4 - \Gamma = f_{\epsilon t} \{ C_{\epsilon 4} [1 - \exp(-l_D^+/C_{d4})]^3$$
$$- C_{\epsilon 5} \exp[C_{A5} E_3 A_3^5] \tanh^2(l_D^+/C_{d5}) \} \varepsilon^2 k$$
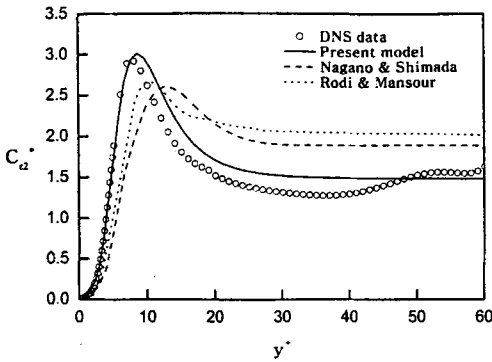$$= - C_{\epsilon 2}^* \frac{\varepsilon^2}{k} \qquad (51)$$

Fig. 12 Comparison of model coefficient $C_{\varepsilon2}^*$ in a plane channel flow, $Re_\tau = 395$
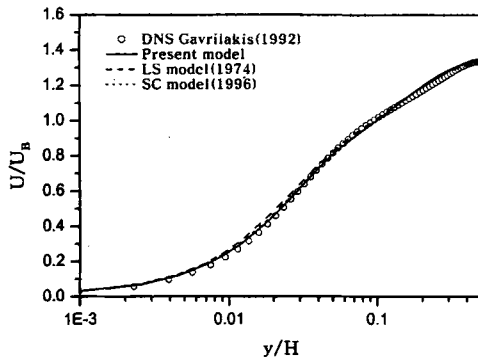

Fig. 13 Comparison of the normalized streamwise velocity profiles predicted by three different ε equation models along the duct wall bisector with the DNS data
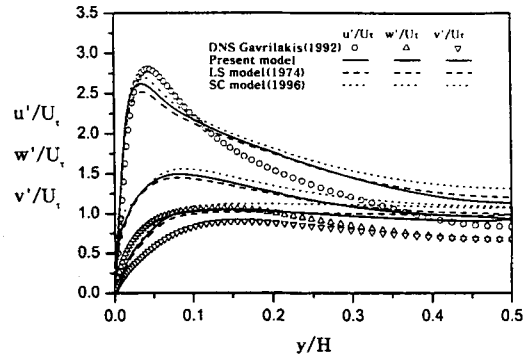

Fig. 14 Comparison of the normalized turbulent velocity distributions predicted by three different ε equation models along the duct wall bisector with the DNS data

Very good agreement between the present equivalent model coefficient $C_{\varepsilon2}^*$ and DNS data are shown in Fig. 12 except some overprediction in the region $7 < y^+ < 50$.

Three different ε equation models [Present, Launder and Sharma(1974), Shin and Choi (1996)] are applied to the simulation of turbulent flow in a straight square duct and the predicted streamwise and turbulence velocities are compared with Gavrilakis' DNS data. Comparison of the normalized streamwise velocity along the duct wall bisector are shown in Fig. 13. In the near wall sublayer, present ε equation model yields the streamwise velocity profile agreed best with the DNS data among the three models. Figure 14 shows the comparison of the normalized turbulence velocities with the DNS data. All the three different ε equation models give large differences

in turbulence velocity distributions from DNS data, but the present ε equation model shows much improved distributions than the predictions from the other ε equation models.

4. Concluding Remarks

A multiple source model for the exact dissipation rate equation in the near wall sublayer is proposed. Each source term is multiplied by wall damping functions to satisfy the limiting conditions as approaching to the wall. We found that the mixed production P_ε^1 was affected by the invariants of small scale turbulence anisotropy e_{ij} and the production by mean velocity gradient P_ε^2 was affected by the invariants of large scale turbulence anisotropy a_{ij}. Since the viscous dissipation term Γ should be balanced with P_ε^1 and P_ε^2 in the near wall sublayer, the amplification functions, $\exp(C_{A5}E_3A_3^5)$ and $\exp(C_{A2}A_3^5)$ were chosen to account for the effects of large and small scale anisotorpies of turbulence to the Γ and P_ε^2 models. Dimensionless distance $y^+ (\equiv y\sqrt{\tau_w/\rho}/\nu)$ is replaced by $l_D^+ (\equiv l_D(\nu\varepsilon)^{1/4}/\nu)$ to extend the low-Reynolds-number k-ε model to the turbulent flow calculations in the arbitrary shaped passage. By introducing the wall damping functions and amplification functions which adopt l_D^+ and invariants of turbulence anisotropies as a function parameter, present multiple source model for the dissipation rate equation can simu-

late the complex near wall behaviors of each source term in the dissipation rate equation very close to the DNS data.

References

Abe, K., Kondoh, T. and Nagano, Y., 1994, "A New turbulence model for Predicting Fluid Flow and Heat Transfer in Separating and Reattaching Flow-. Flow Field Calculations," *Int. J. Heat Mass Transfer*. Vol. 37, No. 1. pp. 139~151.

Gavrilakis S., 1992, "Numerical Simulation of Low Reynolds Number Turbulent Flow through a Straight Square Duct," *Journal of Fluid Mechanics*, Vol. 244, pp. 101~129.

Hanjalic, K. and Launder, B. E., 1972, "A Reynolds Stress Model of Turbulence and its Application to Thin Shear Flows." *J. Fluid Mech.*, Vol. 53, pp. 609~638.

Hanjalic, K. and Launder, B. E., 1976, "Contribution towards a Reynolds-Stress Closure for Low-Reynolds-Number Turbulence," *J., Fluid Mech.*, Vol. 74, pp. 593~610.

Jones. W. P. and Launder, B. E., 1972, "The Prediction of Laminarization with a Two-Equation Model of Turbulence," *Int. J. Heat Mass Transfer* Vol. 15, pp. 301~314.

Kim, J. and Moin, P., 1989, "Transport of Passive Scalars in Fully Developed Channel Flow at Low-Reynolds-Number," *J. Fluids Mech.*, Vol. 177, pp. 133~166.

Laufer, J., 1954, "The Structure of Turbulence in Fully Developed Pipe Flow," *NACA Rep.*, p. 1174.

Townsend, A. A., 1956, *The Structure of Turbulent Shear Flow*, Cambridge University Press, New York.

Launder, B. E., 1989, "Second-Moment Closure ; Present and Future," *Int. J. Heat and Fluid Flow*, Vol. 10, pp. 282~299.

Launder, B. E. and Reynolds, W. C., 1983, "Asymptotic Near-Wall Stress Dissipation Rates in Turbulent Flow," *Physics of Fluids*, Vol. 26, pp. 1157~1158.

Launder B. E. and Sharma B. I., 1974, "Application of the Energy-Dissipation Model of Tur-

bulence to the Calculation of Flow Near a Spinning Disk," *Lett. Heat Mass Transfer* 1, pp. 131~138.

Launder, B. E. and Tselepidakis. D. P., 1991, "Progress and Paradoxes in Modeling Near-Wall Turbulence," *Proc. 8th Turbulent Shear Flow Symposium, Munich*, Vol. 2, 19. 1. 1.

Lay, Y. G. And So, R. M. C., 1990, "On Near-Wall Turbulent Flow Modeling," *J. Fluid Mech.*, Vol. 221, pp. 641~673.

Lumley, L. C. and Khajeh-Nouri, B. T., 1974, "Computational Modeling of Turbulent Transport," *Advances in Geophysics. Proc. 2nd IUGG -IUTAM symp. on Atmospheric Diffusion in Environmental Pollution*, 18A, p. 169

Mansour, N. N., Kim. J. and Moin, P. 1988, "Reynolds-Stress and Dissipation-Rate Budgets in a Turbulent Channel Flow," *J. Fluid Mech.* Vol. 194, pp. 15~44.

Mansour, N. N., Kim. J. and Moin, P., 1989 "Near-Wall k-ε Turbulence Modeling," *AIAA J.*, Vol. 27, pp. 1068~1073.

Nagano, Y. and Shimada, M., 1993, "Modeling the Dissipation-Rate Equation for Wall Shear Flows (Comparison with Direct Simulation Data)," *Trans. JSME (in Japanese)*, Vol. 59, pp. 742~749.

Nagano, Y. Youssef, M. S. and Shimada, M., 1993, "Assessment of ε-Equation for Wall Shear Flows with DNS Database (1st Report, the Case of k-ε Two-Equation Modeling)," *Trans. JSME (in Japanese)*, Vol. 59, pp. 1972~1979.

Patel, V. C., Rodi, W. And Scheuerer, G., 1985, "Turbulence Models for Near-Wall and Low-Reynolds Number Flows: a Review," *AIAA J.* Vol. 23, pp. 1308~1319.

Rodi, W., 1971, "On the Equation Governing the Rate of Turbulent Energy Dissipation," *Rep. TM/TN/A/14, Imperial College of Science and Technology, Department of Mechanical Engineering, London.*

Rodi, W. and Mansour, N. N., 1993, "Low Reynolds Number k-ε Modeling with the Aid of Direct Simulation Data," *J. Fluid Mech.*, Vol. 250, pp. 509~529.